



Sharif, A., Ouyang, J., Yang, F., Chathta, H. T., Imran, M. , Alomainy, A. and Abbasi, Q. H. (2019) Low-cost, inkjet-printed UHF RFID tag based system for Internet of Things applications using characteristic modes. *IEEE Internet of Things Journal*, 6(2), pp. 3962-3975.
(doi:[10.1109/JIOT.2019.2893677](https://doi.org/10.1109/JIOT.2019.2893677))

There may be differences between this version and the published version. You are advised to consult the publisher's version if you wish to cite from it.

<http://eprints.gla.ac.uk/177295/>

Deposited on 08 January 2019

Enlighten – Research publications by members of the University of
Glasgow

<http://eprints.gla.ac.uk>

Low-cost, Inkjet-printed UHF RFID Tag based System for Internet of Things Applications using Characteristic Modes

Abubakar Sharif, *Student Member, IEEE*, Jun Ouyang, Feng Yang, Hassan T. Chattha, *Senior Member, IEEE*, Muhammad Ali Imran, *Senior Member, IEEE*, Akram Alomainy, *Senior Member, IEEE* and Qammer H. Abbasi *Senior Member, IEEE*

Abstract— The radio frequency identification (RFID) has emerged Internet of things (IoT) into the identification of things. This paper presents, a low-cost smart refrigerator system for future internet of things applications. The proposed smart refrigerator is used for automatic billing and restoring of beverage metallic cans. The metallic cans can be restored by generating a product shortage alert message to a nearby retailer. To design a low-cost and low-profile tag antenna for metallic items is very challenging, especially when mass production is required for item-level tagging. Therefore, a novel ultra-high frequency (UHF) radio frequency identification (RFID) tag antenna is designed for metallic cans by exploiting the metallic structure as the main radiator. Applying Characteristics mode analysis (CMA), we observed that some characteristic modes associated with the metallic structure could be exploited to radiate more effectively by placing a suitable inductive load. Moreover, a low cost, printed (using conductive ink) small loop integrated with meandered dipole used as an inductive load, which was also connected with RFID chip. The 3-dB bandwidth of the proposed tag covers the whole UHF band ranging from 860 - 960 MHz when embedded with metal cans. The measured read range of the RFID tag is more than 2.5 meters in all directions to check the robustness of the proposed solution. To prove the concept, a case study was performed by placing the tagged metallic cans inside a refrigerator for automatic billing, 97.5 % tags are read and billed successfully. This study paves the way for tagging metallic bodies for tracking applications in domains ranging from consumer devices to infotainment solutions, which enlightens a vital aspect for the Internet of Things (IoT).

Index Terms— Characteristic mode theory (CMT), Internet of Things (IoT), radio frequency identification (RFID) tag antenna, smart refrigerator

I. INTRODUCTION

The Internet of Things foresees a future in which physical and virtual things can be uniquely identified on a global scale by means of emerging integrated wireless technologies.

A. Sharif, J. Ouyang, and F. Yang are with the School of Electronics Science and Engineering, University of Electronic Science and Technology of China, Chengdu 611731, China (Corresponding author: Jun Ouyang.)

H. T. Chattha, is with Department of Electrical Engineering, Faculty of Engineering, Islamic University in Madinah, Madinah, Saudi Arabia

A. Alomainy is with Queen Mary University of London, United Kingdom

Q. H. Abbasi and M. Imran are with the Department of Electronics & Nanoscale Engineering, University of Glasgow, and Glasgow, UK

(E-mail: yjou@uestc.edu.cn; sharifuestc@gmail.com, Qammer.abbasi@glasgow.ac.uk)

After the Internet, the IoT is regarded as an economic wave with emerging applications like smart cities, connected vehicles, smart healthcare monitoring, smart shopping and etc. The IoT is producing a paradigm shift by integrating numerous technologies such as RFID, sensors, 5G and other smart technologies, which enables communication between digital and physical entities. With this growing era of the Internet of Things (IoT), radio frequency identification (RFID) technology has opened a new paradigm especially in combination with IoTs [1-10].

RFID is one of vital technology which transforms IoT into the identification of things by enabling a device to share its unique digital code through a wireless network [11]. Both technologies have been emerging into many new applications [11-12] from consumer electronics to entertainment. However, there are many applications in which effective automatic identification technology is still very crucial. The ultra-high frequency (UHF) RFID tags are more suitable for many applications such as retail management, supply chain and sensing due to their long-read range and low-cost. The wide range of daily life applications requires tagging of many different materials such as metals, wood, glass and so forth. The sensitivity towards tagging materials is one inherited problem associated with UHF tags. The metallic objects are considered to be more crucial for tagging due to completely different boundary conditions [13-15]. The performance of UHF RFID tags seriously degraded near the proximity of metals regarding detuning of the frequency band and reduction in gain of the antenna. In some recent years, many solutions have been proposed for tagging metallic objects [16-21].

However, to reduce the influence of the metallic objects, most of the tags reported in literature utilize microstrip patch-like structure, which employs a ground plane beneath the substrate of the antenna. These microstrip patch antennas are not suitable for item-level tagging because of their large size and more cost. Moreover, the presence of metallic items in supply chain goods makes it more challenging to tag these objects. This challenge is magnified further when tagging of metallic objects involved at item-level instead of bulk, because of their low cost and small size requirements. Therefore, to meet these requirements, it was an arduous task to design a UHF tag for item-level tagging of metallic cans at large scales.

In this paper, metallic objects chosen for tag design are metallic cans which are very common in daily life and supply chain such as soft drinks. In literature, there are very few tags reported for tagging metallic cans [21-23] including some commercially available solutions [24-26]. In [21], a circular

microstrip UHF RFID tag fabricated on double-sided copper clad FR 4 board was proposed. Such a circular microstrip tag was designed to fit in the bottom cavity of the metallic can as shown in Fig. 1(b) and 2. This location was chosen to solve the problem of packing half dozen metallic can together as shown in Fig. 2. However, the disadvantages associated with circular microstrip tag are its high cost for item-level tagging and small read range just 0.23 meters. A sprayed antenna using conductive paint proposed in [22] for 5.8 GHz radio frequency identification wireless LAN (RFID_WLAN) application. The antenna was fabricated by sandwiching it between thin layers of sprayed paint. This antenna with a large footprint was difficult to fabricate and possess a very narrow bandwidth (impedance match with RFID chip) with small read range.

Furthermore, as referred in [23], [24], Toyo Seikan Kaisha, LTD. has developed RFID equipped metallic can by exploiting the tab ring and the space between tab and lid as an antenna and connected it with RFID chip (tab ring is shown in Fig. 2). This solution is a good option considering size requirements of RFID tags. However, this will create a problem when the metallic can packs stacked over each other. Moreover, its fabrication complexity is more due to the small footprint of tag.

Therefore, in order to overcome the aforementioned challenges, characteristics mode theory (CMT) in combination with CMA was used for the first time in literature for designing a suitable tag antenna for tagging metallic cans and finding the right location for placing the tag. By using CMA, we present a tag design for metallic items by identifying that there is already a tag antenna in metallic objects, we just exploit it to work more efficiently. It is quite similar as quoted by Italian sculptor Michelangelo "The sculpture is already complete within the marble block, before I start my work. It is already there; I just have to chisel away the superfluous material". In recent years, CMA in combination with CMT becomes a prevalent tool in antenna design and fabrication. CMT provides physical insight to antenna design by splitting radiation characteristics of the antenna into different modes. Furthermore, it provides the resonance frequency and optimal location to excite or suppress some specific modes [27-30]. As expressed in [31], [32] by Martens et al., the desired modes can be excited using inductive coupling element (IDE) or capacitive coupling elements (CCE) at selected locations.

Therein literature there are few designs reported for RFID tag antenna designs using Characteristics mode analysis [35]–[39]. In [36], the car number plate structure was exploited to make it a long-range RFID tag antenna by using CMA and pattern synthesis technique. As presented in [37], a metal plate of size (150x80mm²) can be converted to RFID tag by placing small inductive load mounted on high permittivity ceramic substrate. However, this solution is not suitable for metallic can due to its high-cost ceramic material and high volume of the inductive element.

In this paper, we present a low-cost smart refrigerator system for future internet of things applications. The proposed smart refrigerator is used for automatic billing and restoring of beverage metallic cans. For commercial deployments of this system, it was very challenging to design a low-cost tag for metallic cans. Therefore, we also design a novel RFID tag antenna design for tagging beverage metallic cans. The proposed tag exploits the structure of metallic can as the main

radiator using CMA. Some selective modes of the metallic can be excited by placing ICE at current maxima of most significant mode (with more modal significant value), that contributes the most towards radiation. A low-cost, conductive ink printed small loop antenna integrated with dipole was used to work as an inductive load and was attached to provide a match with RFID chip. The 3-dB bandwidth of proposed tag embedded with metal can cover whole UHF band ranging from 860 - 960 MHz (Covering the three major UHF RFID bands, the European region band (860–870 MHz) and the American/Asian region bands (900–960 MHz)). Moreover, the simulated gain of RFID tag is more than 3.2 dBi for the whole UHF RFID band. This tag is fulfilling the requirements of low cost and size compactness.

Furthermore, the antenna is also fabricated by embedding it within thin layers of sprayed paint, to hide or embed the tag inside the product and further to use the extra space provided by the tag for logo printing and other advertisement printing purposes. Therefore, this tag can be used for tagging beverage metallic cans on a large scale. The read range is measured using Tagformance Pro setup for one RFID equipped metallic can. To investigate it further, the read range is also measured using Handheld RFID Reader for one metallic can and a pack of half dozen metallic cans. This experiment shows the potential application of this tag for conveyor belt applications. Furthermore, an experiment of auto billing of the metallic can was connected by placing the tagged metallic can inside a refrigerator. The customers can open the door of the refrigerator by scanning the displayed QR code using online payment applications. Moreover, the customers can choose any product of their own choice, and the money will be deducted from their online payment account.

This work is the pioneer in designing a tag antenna for item-level tagging metallic objects using CMA. Our contribution is listed as follows:

- 1) We propose a low-cost tag for item-level tagging of metallic cans by exploring its characteristics modes using CMA.
- 2) An optimal probe and location for tagging metallic is achieved by analyzing the normalized model weighting coefficient (MWC) amplitude.
- 3) To the best of our knowledge, we are first to propose a low-cost RFID based smart refrigerator system to test the proposed tag commercially by demonstrating the idea of automatic billing of metallic cans along with some other products.
- 4) A unique feature is implemented by counting the tagged products and generating an alert message for retailer to place more products, if a certain product is less than a threshold (taken as 10 in our case), this experiment shows a potential to revolutionize the IoT industry and supply chain management by providing item-level tracking of goods for effective decision-making.
- 5) Another experiment is demonstrated by attaching a trash bin with refrigerator, an RFID reader antenna is house at wall of trash bin; the trash bins is used for collecting the empty metallic cans and return a small incentive to customers by reading the tag mounted on can. which

paves a cost effective and environment friendly solution by reutilizing unfilled metal cans.

The rest of paper is organized as follows. In section II, actual practical application requirements are discussed. In section III, characteristic mode theory and characteristic mode analysis of Metallic can is elaborated in detail. In section IV, the choice of Inductive loop with MWC is explored. In section V simulation and measurement results are presented. In section VI, Automatic billing cabinet experiment and conveyer belt reading experiments are discussed. Finally, the conclusion is drawn in section VII.

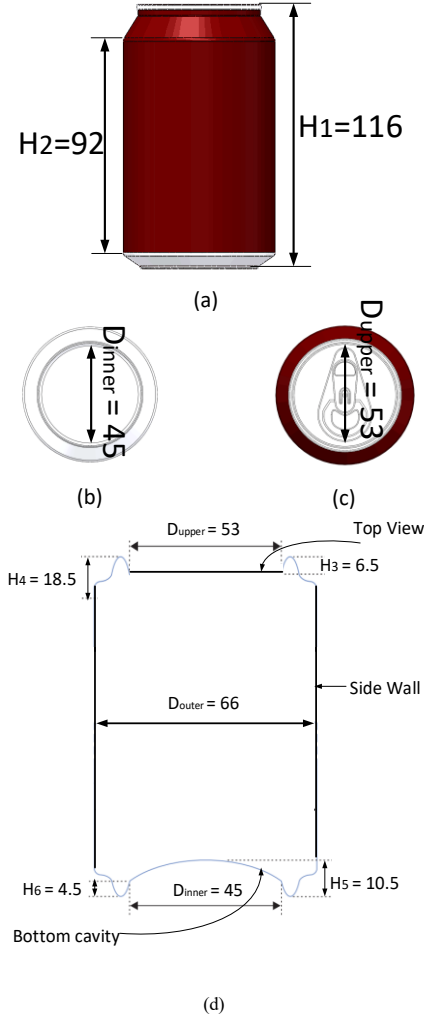


Fig. 1. Geometry and dimensions of simulated metallic can Modal (a) front view (b) bottom cavity (c) top view (d) Layout and detailed dimensions of Metallic Can

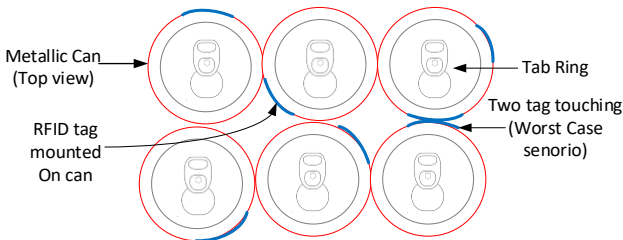


Fig. 2. Packing arrangement of half dozen metallic Can (Top View) with different scenarios of attaching RFID tag on the cylindrical side wall

II. APPLICATION REQUIREMENT

Fig. 1 shows the dimensions and geometry of 330 ml metallic can, commonly used for beverages such as beer and soft drinks. Because of the massive scale tagging of the metallic can at item-level requires an RFID tag that must fulfill following practical application Requirements:

- Low cost, low profile and printable for item-level tagging
- The actual dimensions of the metallic can should not be changed
- A location to place the tag, where it can be read independently inside a pack of half dozen metallic cans (as shown in Fig. 2)

From, Fig. 1, there are three possible locations for tag attachment: i) attach the tag at the top of the metallic can. However, this place is not suitable, if two metallic cans are stacked over one and other ii) install the tag at bottom cavity, but in this case, it is difficult to read the tag in some scenarios such as conveyer belt application or while stacking the metallic can packs over one another iii) cylindrical wall of metallic can, however, in this case, the tags cannot able to work, while packing half dozen metallic cans as shown in Fig. 2. Furthermore, there will be a worst-case scenario when two adjacent tags touch each other. Therefore, an RFID tag should be proposed and attached to the location to solve the problem mentioned above, while keeping in mind the low cost and other item-level requirements.

In this paper, cylindrical side wall for tag attachment was chosen carefully while addressing aforementioned issues.

III. CHARACTERISTIC MODE ANALYSIS

A. Characteristics Mode Theory (CMT)

Characteristic modes can be defined as current modes calculated numerically for some arbitrary shaped conducting bodies. These current modes entirely depend on the shape and size of conducting objects and are independent of any feed or excitation source. Moreover, characteristic modes (CM) can be obtained by solving eigenvalue equations, inferred from Method of Moments (MoM) based impedance matrix as follows [18-20]:

$$X \left(\vec{J}_n \right) = \lambda_n R \left(\vec{J}_n \right) \quad (1)$$

Where λ_n are the eigenvalues, \vec{J}_n are eigen currents or eigenfunctions, and are real and imaginary components of MoM impedance matrix respectively.

As CM form an orthogonal set of functions, so, the total current on the surface of the antenna or radiating object can be expressed as a linear superposition of these characteristic mode currents as follows [18-20]:

$$J = \sum_n \alpha_n J_n = \sum_n \frac{V_n^i J_n}{1 + \lambda_n} \quad (2)$$

Where α_n is the complex modal weighting coefficient (MWC) associated with each mode and can be calculated as follows [18-20]:

$$\alpha_n = \frac{V_n^i}{1 + \lambda_n} = \frac{\langle E^i, J_n \rangle}{1 + \lambda_n} \quad (3)$$

The term V_n^i refers to as modal excitation coefficient (MEC) and can be defined as [20]:

$$V_n^i = \langle E^i, J_n \rangle = \iint_S J_n * E^i dS \quad (4)$$

Furthermore, the modal significance (MS) can be defined as [20]:

$$MS = \left| \frac{1}{1 + \lambda_n} \right| \quad (5)$$

The modal significance is a key feature associated with each CM because it provides information about the coupling capability of each CM with the external excitation source.

The combination of modal signification and modal excitation coefficient provides the measure of the contribution of each characteristic mode in total electromagnetic response to a given external excitation source.

B. Characteristics Mode Analysis of Metal Can

Fig. 3 shows the mesh views of the metallic can using 6230 flat triangles with Rao-Wilton-Glisson (RWG) basis functions. The characteristics mode analysis is performed using an in-house written MATLAB code with mode tracking algorithm. The eigenvalues plot for the first six modes of metallic can be obtained by using the in-house program as shown in Fig. 4. Moreover, the plot of modal significance associated with each mode is shown in Fig. 5. It is clear that (from Fig. 4) characteristic mode 1 (CM1), characteristic mode 2 (CM2) and characteristic mode 3 (CM3) have small eigenvalues (<10), which shows their high radiation capability as compared with other modes.

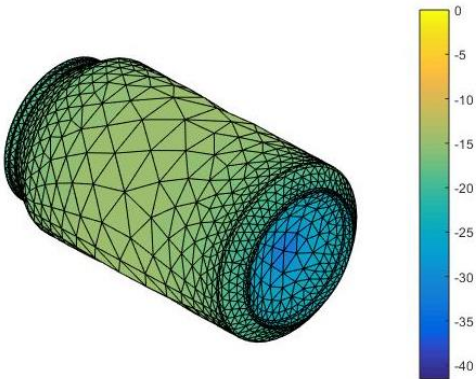


Fig. 3. Mesh view of the metallic can with 6230 flat triangles

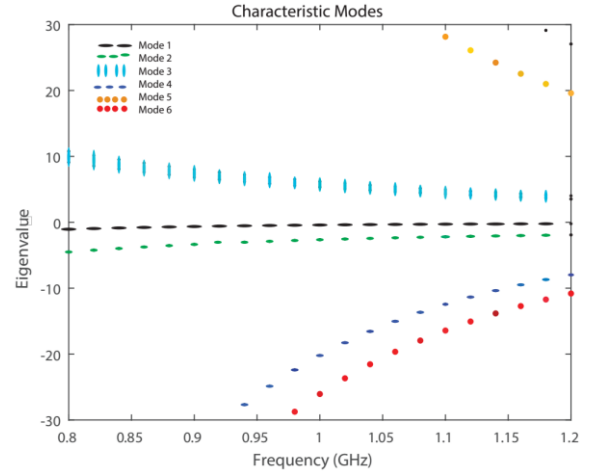


Fig. 4. Eigenvalues of characteristics modes of the metallic can as a function of frequency

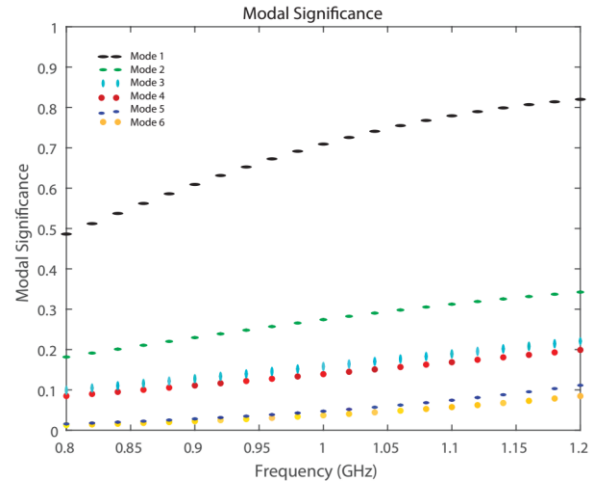


Fig. 5. Modal signification plot of characteristic modes of the metallic can

This fact can be clarified further from modal significance plot associated with characteristic modes that mode 1 has more modal significance value of about 0.7 at 915 MHz. Hence, at 915 MHz, CM1 dominates and exhibits more radiation capability as compared with other modes. The CM4 and CM6 exhibit capacitive behavior with eigenvalues (<10). Moreover, the CM4 and CM6 have a modal significance about 0.1 and 0.05 respectively, which describes their less radiation ability. Furthermore, the CM3 and CM5 show inductive behavior because their eigenvalues are greater than 0.

Furthermore, to analyze the different characteristic modes more precisely, the characteristics currents and associated far field of each mode are studied. Fig. 6 shows characteristic mode current and associated far field of first six modes of the metallic can at 915 MHz. It is clear that CM1 and CM4 can radiate more effectively with omnidirectional radiation pattern. Moreover, the current distribution of CM1 has maxima at the middle of metallic can, which makes it more favorable for placing a load to activate this particular mode.

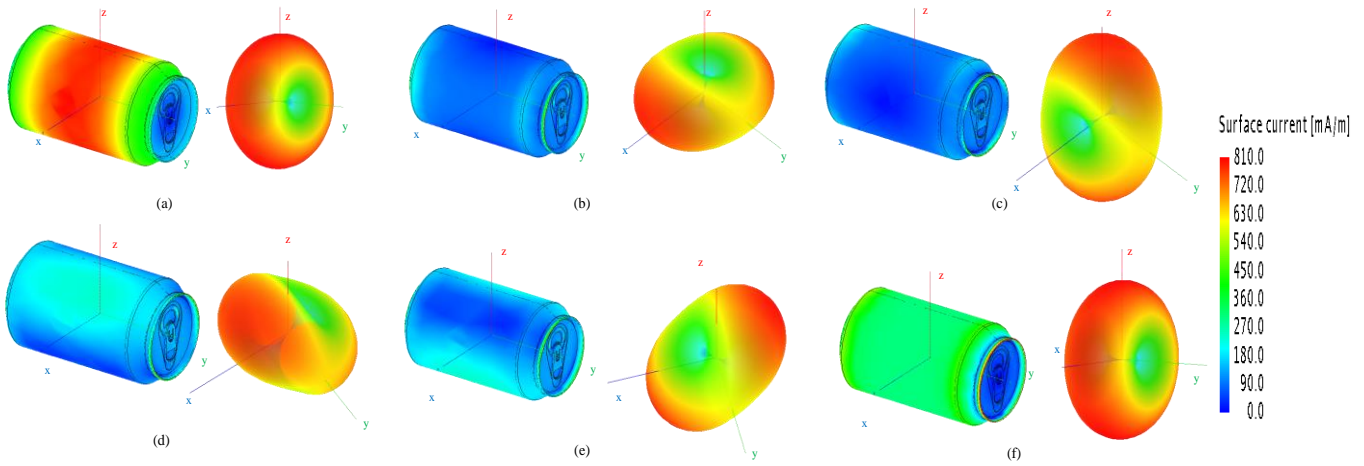


Fig. 6. Mode current distribution and far-field associated with different modes of metallic can, (a) CM₁, (b) CM₂, (c) CM₃, (d) CM₄, (e) CM₅, (f) CM₆

Similarly, the CM6 has a similar far-field characteristic as CM1. However, the current distribution of CM6 is different from CM1. The current maxima of CM6 lie on the edge of the upper cavity. Moreover, the CM6 current is not symmetrical along the whole cylindrical surface. While on the other hand, the CM2, CM3, CM4, and CM5 asymmetric current distribution along xz and yz plane (as shown in Fig.6).

Hence, they will contribute very less if CM1 is mainly excited using an inductive load or capacitive Load. Additionally, we can excite CM1 partially by placing a load, at the upper edge of the cylindrical surface. This will give rise to two types of current distributions as shown in Fig. 7: i) Current distribution 1, This current distribution is mainly due to the CM1, which contributes more towards radiation due to its more modal significance ii) Current distribution 2: this current distribution corresponds to CM4 and CM6, which will also contribute to the radiation far-field partially, when CM1 will be excited.

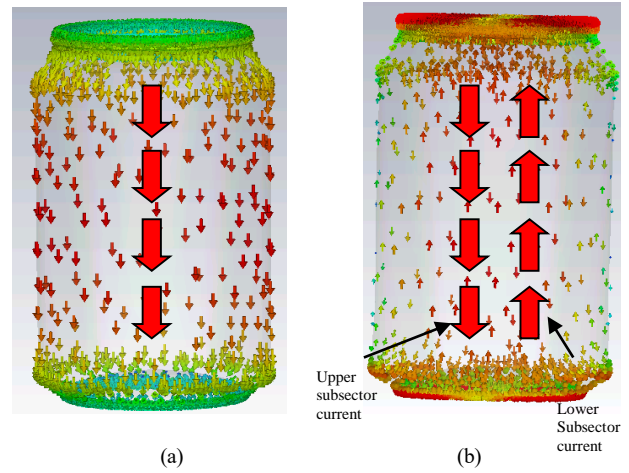


Fig. 7. Two types of characteristic mode current directions
(a) Current distribution 1(mode 1) (b) Current distribution 2(mode 4 & 6)

In light of the aforementioned current distribution, we can calculate the MWC of each excited mode. By exploiting the symmetry of current distribution, the following expansion can be expressed as follows [18-20]:

$$\begin{bmatrix} e^{j\beta} \\ 1 \end{bmatrix} = k_1 \begin{bmatrix} 1 \\ 1 \end{bmatrix} + k_2 \begin{bmatrix} 1 \\ -1 \end{bmatrix} \quad (6)$$

Where “1” and “-1” depicts the current in upper sector of the cylindrical wall and current in lower sector of cylindrical wall respectively as shown in Fig. 7.

The expression (6) can be solved as follows:

$$\begin{cases} k_1 = \frac{e^{j\beta} + 1}{2} \\ k_2 = \frac{e^{j\beta} - 1}{2} \end{cases} \quad (7)$$

Where β is the phase difference of different current distribution associated with each characteristic mode.

To get MWC, we have to substitute (7) and (4) into (3) as follows:

$$\alpha_n = \frac{\langle J_n, E^i \rangle}{1 + j\lambda_n} = k_1 \frac{J_n(P)}{1 + j\lambda_n}; \quad n = 1 \quad (8)$$

$$\alpha_n = \frac{\langle J_n, E^i \rangle}{1 + j\lambda_n} = k_2 \frac{J_n(P)}{1 + j\lambda_n}; \quad n = 4, 6 \quad (9)$$

By exploiting the orthogonality of characteristics modes, the total current on the surface of the metallic container can be expressed as a sum of selectively excited mode currents using (2) as follow [20]:

$$J = \sum_n \alpha_n J_n = \sum_n \frac{V_n^i J_n}{1 + \lambda_n} \approx \alpha_1 J_1 + \alpha_4 J_4 + \alpha_6 J_6 \quad (10)$$

Similarly, the total far field can be expressed as a superposition of far-field contributed by each independent CM mode using (5) as expressed below:

$$E = \sum_n \alpha_n E_n \approx \alpha_1 E_1 + \alpha_4 E_4 + \alpha_6 E_6 \quad (11)$$

IV. DESIGN OF INDUCTIVE COUPLING ELEMENT (ICE)

As discussed in [21], [22], some specific modes can be excited independently using ICE or CCE. The ICE must have to place at current maxima of a particular mode to excite that specific mode, on the other hand, the CCE should be placed at current minima to excite that specific mode [21].

Furthermore, it is advantageous to excite a specific mode using ICE. By using ICE, the specific mode can be excited purely even when they are approaching close to their modal resonance [21]. In this RFID tag design application, the ICE also provides another advantage of conjugate matching with a capacitive impedance of RFID microchip. Fig. 8 shows some alternative ICE to act as an RFID tag, to excite particular characteristics mode when attached to the metallic can. The ICEs consist of typical RFID tag structure: a loop, meander line structure and capacitive plates at both ends. The lower plate should be attached to the metallic can.

The ICE1 is designed and optimized based on three main aspects 1) electrical properties: electrically small, imaginary impedance match over UHF RFID band 2) fabrication complexity: dimensions are optimized so that it can't be bent when attached to metallic can 3) cost: low cost and low-profile for mass production. Design optimization is performed using CST Microwave Studio. The ICE1 shown in Fig. 8 (a) consists of a matching loop, meander line structure and capacitive plates at both ends. The matching loop is designed and optimized to provide an imaginary impedance of 100 to 120 Ohms in UHF RFID band, which is necessary for conjugate matching with RFID chip. The meander line structure at both sides of loop helps to reduce electrical length. The ICE1 is loaded with capacitive plates, further to reduce the electrical length of the antenna and facilitate impedance matching.

The length of lower plate is deliberately kept more than upper plate, because it will be used to excite CM1. The ICE1 has two main advantages over other ICEs such as i) its upper meandered length is 12 mm, which is less than upper cavity wall (represented by H4 in Fig. 2), so the actual dimensions of the metallic can will not be affected. ii) Its lower plate has the longest dimensions among other tags, so it can excite CM1 more efficiently as compared with other ICEs. Other ICE2 as shown in Fig. 8 (b) can be used to get other advantages such as reusable tag; if someone tries to remove it from the product, its connection can be easily broken from the chip. Furthermore, ICE3 and ICE4 can give the advantage of flexibility in conjugate matching with various RFID chips by changing the dimensions of the loop. Fig. 9(a) and (b) represent the simulation modal of the metallic can along with the position of mounting ICE at the upper edge and at the middle of can.

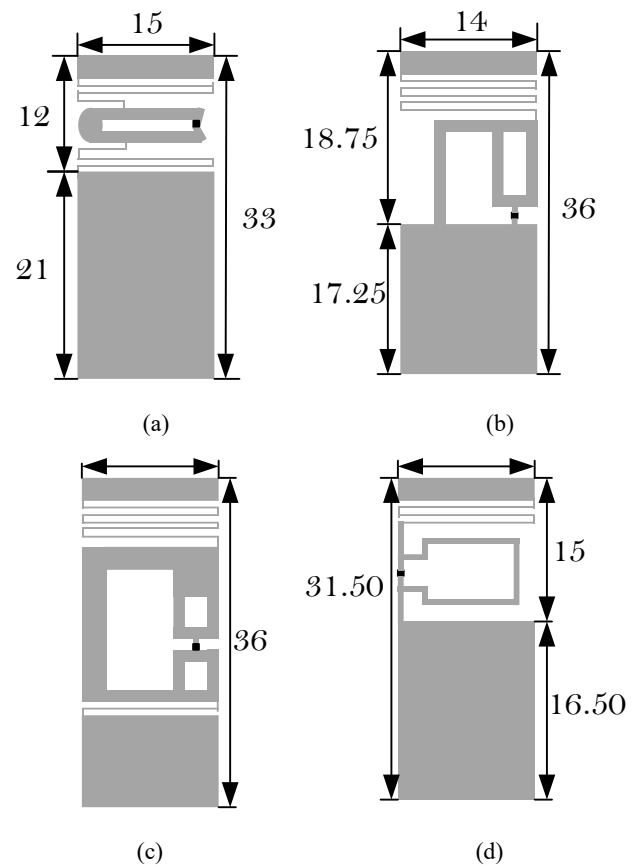


Fig. 8. Dimensions of alternative inductive loads attached with RFID chip (a) ICE₁ (b) ICE₂ (c) ICE₃ (d) ICE₄

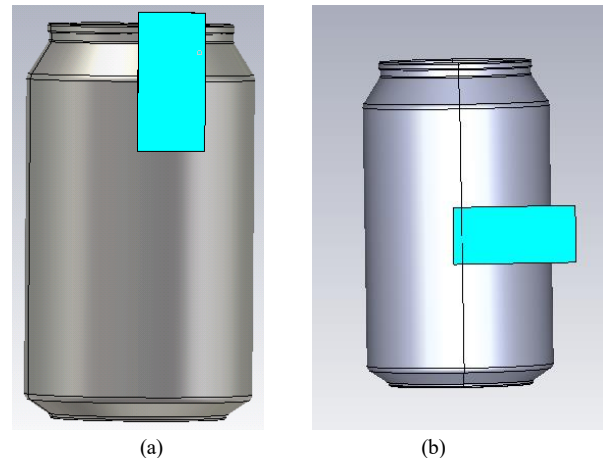


Fig. 9. Simulation modal of the metallic can (a) with ICE @ upper Edge (b) with ICE at middle of metallic can

In addition to this, the choice of the optimal probe (ICE) and optimal position of ICE on metallic can is further explained using MWC. The characteristic modes performance comparison for four ICEs in normalized MWC amplitude is shown in Fig. 10. This comparison is performed after attaching all ICEs at the upper edge of metallic can. In particular, all ICEs exciting CM1 and CM4, whereas ICE1 outperforms the other ICEs in terms of exciting CM1. Additionally, it is worth to mention that CM1 is most significant mode of metallic can.

Therefore, ICE1 is optimal choice in terms of cost, size and mode excitation efficiency. As far as concerned with the optimal position for mounting ICE1, the comparison of normalized MWC amplitude after mounting ICE1 at upper edge and middle position of metallic can is shown in Fig. 11. It is clear from MWC amplitude, at the middle position, the CM1 excites more efficiently, with more mode excitation purity. However, at upper edge, the ICE1 excites CM1 partially along with CM4. Although, the middle position is optimal position for placing ICE1 to excite CM1, but this position is not favorable from our application perspective. Because, at middle of can, the ICE1 can be more prone to damage or to be de-attached from metallic can. Moreover, this position is not favorable for bulk tagging or refrigerator based applications. Therefore, the ICE1 is mounted at upper edge to partially excite the CM1, even though it is not the optimal position to excite CM1, but it fulfils our application requirements along with satisfactory read range.

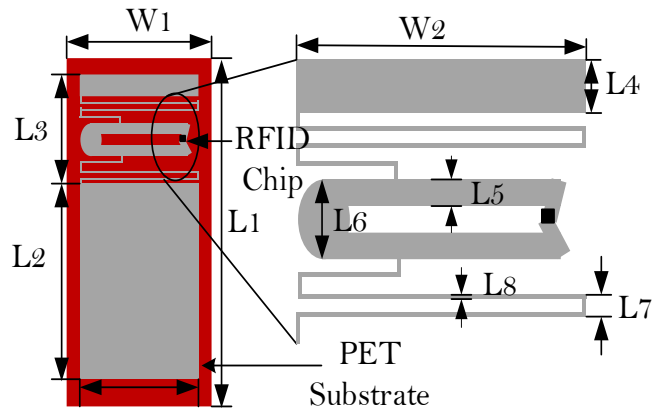


Fig. 12. Detailed dimensions of ICE₁ (used for RFID tag configuration)

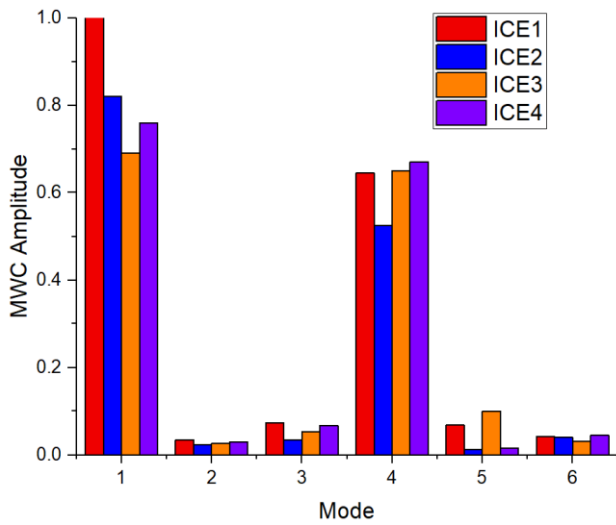


Fig. 10. Comparison of the normalized MWC amplitude of Four ICEs

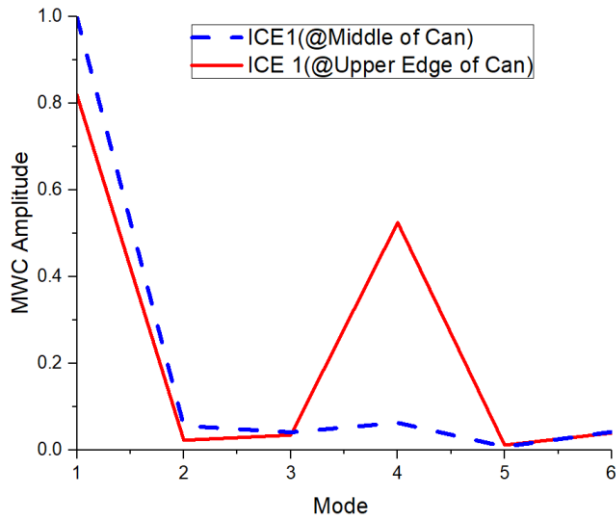


Fig. 11. Comparison of the normalized MWC amplitude for ICE₁ mounted at two different positions of metallic can



(a)



(b)

Fig. 13. (a) ICE₁ fabricated on a PET substrate and mounted on Metallic can (RFID tag configuration) (b) ICE₁ embedded between paint layers mounted on Metallic can

V. SIMULATION AND MEASUREMENTS

The detailed dimensions of ICE1 are depicted in Fig. 12. The values of dimensions of ICE1 are listed in Table II. The ICE1 was fabricated on $100\ \mu\text{m}$ PET substrate using conductive ink ($15\ \mu\text{m}$ Silver with $\sigma = 12.5 \times 10^6\ \text{S/m}$) by an ink-jet printer (as shown in Fig. 13). The ICE1 mounted on the metallic can (proposed RFID tag) is simulated using CST Microwave studio with a whole bottom plate attached to the metallic can to excite CM1. Fig. 13(a) shows the RFID tag (ICE1 mounted with metallic can) fabricated using PET substrate, and a glue layer used for pasting the ICE1 on the metallic can. Although the ICE1 is small enough to be mount at any space on the metallic can, still it can cover some information printed on metallic can. However, to address this issue, the tag is also fabricated by embedding the tag between $100\ \mu\text{m}$ paint layers ($\epsilon_r = 6.5$) as shown in Fig. 13(b). The RFID tag antenna fabricated by embedded in thin paint layers can be used to hide or embed the tag inside the product and further to use the extra space provided by tag for logo printing and other advertisement printing purposes.

The performance of RFID tag fabricated using paint layers is almost the same as for simple PET substrate-based RFID tag. This fact further supports that this tag is a potential candidate for the hiding or embedding it inside a product using paint layer since paint layer has no significant effect on the performance of tag. Fig. 14 shows the simulated results of the impedance of individual ICE1. The imaginary impedance of ICE1 is ranging from 90 Ohms to 110 Ohms for whole UHF RFID band (860 - 960 MHz). Moreover, the real impedance of individual ICE1 is very low ranging from 0.01 Ohms to 0.2 Ohms for whole UHF band. Fig. 15 represents the simulated and measured results of the impedance of proposed RFID tag after mounting on the metallic can. It is clear that after mounting the ICE1 to a metallic can, there is an increase in imaginary impedance ranging from 130 to 150 Ohms.

Moreover, the real impedance also increases ranging from 6 Ohms to 8 Ohms. The impedance of the proposed RFID tag can provide a suitable match with Impinj Monza R6 RFID chip having impedance $14\text{-}140\ j$ at 915 MHz (calculated by simulating equivalent circuit of the chip using ADS). Also, the measured imaginary impedance of the proposed tag is quite similar to the simulation results. However, the measured real impedance is slightly less than simulated real impedance, which may be due to the difference in permittivity and height of PET material used for printing of ICEs.

The simulated and measured return loss of proposed RFID tag after mounting on the metallic can is shown in Fig. 16. The simulated return loss shows a 3-dB bandwidth ranging from 860-960 MHz. As expressed in [16], the 3-dB return loss is enough for RFID applications due to high radiation capacity of proposed RFID tag. However, the measured return loss of proposed RFID also gives 3 dB return loss for whole UHF RFID band with a slight shift. The shift can be either to glue layer used to paste the tag on the metallic can or some fabrication tolerance or due to discrepancies in measurement procedure.

Table II. Layout and dimensions of ICE₁

| Dimension | L1 | L2 | L3 | L4 | L5 |
|------------|----|-----|-----|----|------|
| Value (mm) | 36 | 18 | 12 | 2 | 1 |
| Dimension | L6 | L7 | L7 | W1 | W2 |
| Value (mm) | 5 | 1.5 | 0.5 | 18 | 15.5 |

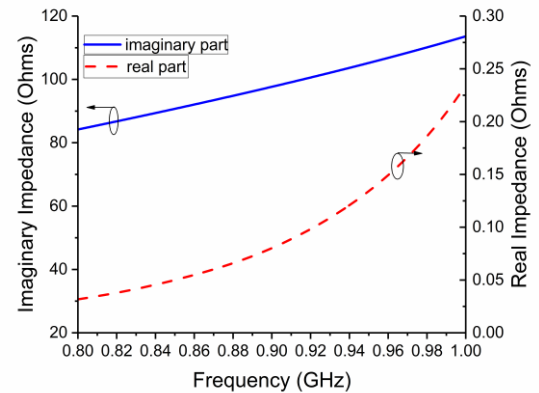


Fig. 14. The simulated impedance plot of individual ICE₁

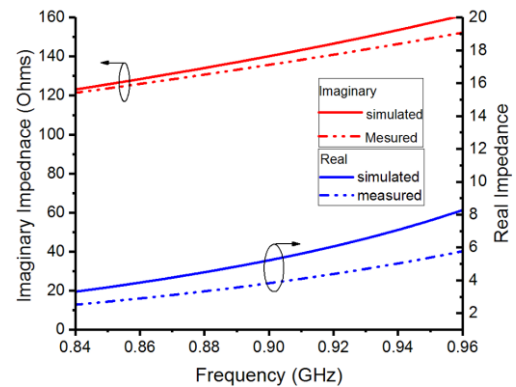


Fig. 15. Simulated and measured results of the impedance of proposed RFID tag after mounting on metallic can

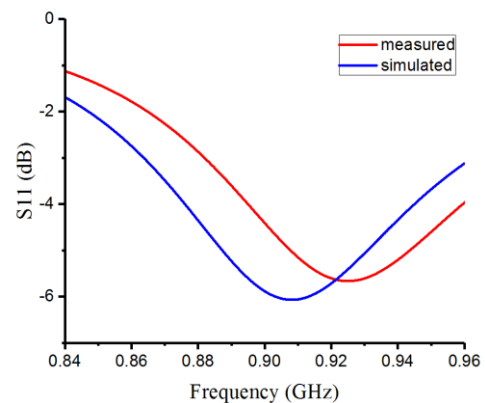


Fig. 16. Simulated and measured return loss of proposed RFID tag after mounting on metallic can

Furthermore, the 3D gain radiation pattern of individual ICE1 is shown in Fig. 17 (a). The individual ICE1 proposes a very low gain because of its small size. Moreover, it does not provide a good Omni-directional pattern as desired in this application. This individual ICE1 placed on metallic cylinder to excite CM1 mode partially. Although, the current maxima of CM1 is located in the middle of the cylinder, but still CM1 can be excited partially with the load, placed in the position shown in Fig. 9. The purity and efficiency of CM1 can be increased by placing the load at the center or by increasing the length of ICE at the expense of cost and size of ICE (as shown by the other ICEs). This can be proved from the radiation pattern of proposed RFID tag after mounting it on the metallic can. The radiation pattern of proposed RFID tag after mounting on the metallic cylinder is shown in Fig. 17(b). The value of gain improves up to 3.21 dBi as compared with individual ICE1 gain and results in Omni- Directional as required in this application. The radiation pattern in Fig. 17 shows that the ICE1 excites CM1 partially. Furthermore, after mounting ICE1 at this position will also excite partially CM4 and CM6, which have very less radiation capacity as compared with CM1.

To verify it further, the correlation coefficient ρ is calculated to describe the analogy between full wave radiation pattern and radiation pattern of CM1 using [20]:

$$\rho = \frac{\left| \iint_{\Omega} E_{CM} \cdot E_{full_wave}^* d\Omega \right|}{\sqrt{\iint_{\Omega} |E_{CM}|^2 d\Omega} \sqrt{\iint_{\Omega} |E_{full_wave}|^2 d\Omega}} \quad (12)$$

Where E_{CM} describes the far field of characteristic modes obtained using Characteristic mode analysis (CMA), E_{full_wave} is far-field obtained using full-wave simulation software CST and Ohmz is solid angle.

The correlation coefficient ρ obtained using (12) gives a value of 0.9210 at 920 MHz, which proves a good similarity between the far-field pattern of proposed RFID tag and CM1 of the metallic can. Moreover, the far-field pattern is little bit different from pattern of ICE1, which is due to excitation of CM4. The far-field pattern also shows little bit inclusion of CM4 pattern. For RFID applications, the read range is an important parameter. The theoretical read range (r) can be obtained using Friis equation as follows [4]:

$$r = \frac{\lambda}{4} \sqrt{\frac{P_r G_r G_a \tau}{P_{th}}} \quad (13)$$

Where P_r is power transmitted by RFID reader, G_r is gain of RFID reader, G_a is gain of proposed RFID tag, and P_{th} is minimum threshold power of RFID microchip.

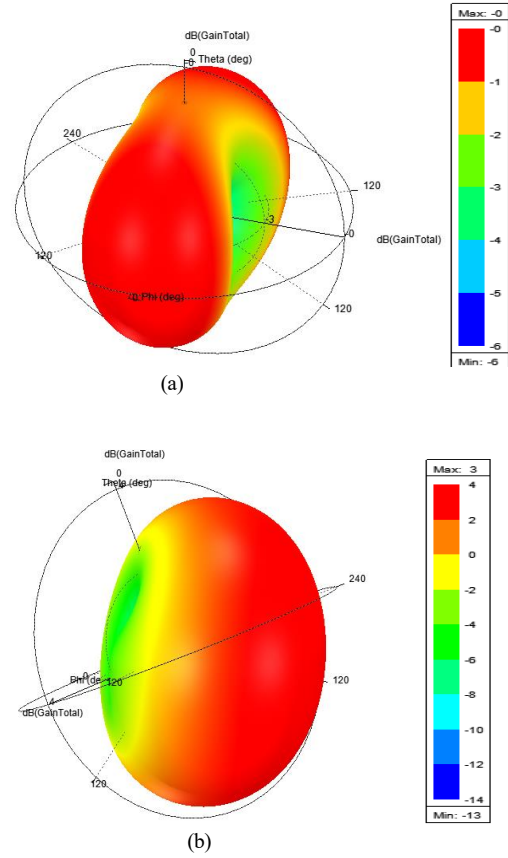


Fig. 17. (a) Simulated 3 D gain radiation pattern of ICE₁ (b) Simulated 3 D gain radiation pattern of ICE₁ after mounting on the metallic can at current maxima

However, another more practical and efficient method for read range estimation is to calculate maximum read range with the maximum permitted Equivalent Isotropically Radiated Power (EIRP) (typical value is 4W), and then estimates the read range for the small value of EIRP at a fixed distance as expressed by (14).

$$r_{max} = r_{ref} \sqrt{\frac{EIRP_{max}}{EIRP_{ref}}} \quad (14)$$

Where r_{max} and r_{ref} are maximum read range of RFID tag and reference read range obtain at fix distance measure in a lab environment, respectively. Moreover, $EIRP_{max}$ is the maximum permitted value of EIRP (which is typically 4 W), and $EIRP_{ref}$ is reference EIRP of read range measuring equipment.

A read range measurement set up based on Tagformance pro device from Voyantic Company is deployed to measure the maximum read range of RFID tag in a lab environment as illustrated in Fig. 18. The setup also consists of the linear polarized antenna (6 dBi gain), a foam spacer and laptop computer install with software to plot the measured read range. A frequency sweep is run using Tagformance device. Foam spacer specifies the fixed distance (r_{ref}) between RFID tag and reader antenna. The theoretical read range estimated using (14).

The theoretical read range of the tag measured from different directions such as front, back, top and bottom. Fig. 19 represents the theoretical read range measured using Tagformance setup. The tag has read range of more than 2.5 meters for the whole frequency band ranging from 860 - 960 MHz (Covering the three major UHF RFID bands, the European region band (860–870 MHz) and the American/Asian region bands (900–960 MHz)).

As mentioned earlier, if a simple inlay or microstrip tag designed for cylindrical wall, it will not able to work in case of half dozen metallic can pack as mentioned in Fig. 2. Since in our case, the whole body of the metallic can is working as a radiator. Therefore, this tag can be read from any direction. So, this RFID tag can also work for tagging half dozen packs. In addition, the read range RFID tag is measured using a simple handheld reader after mounting ICE1 on half dozen pack of the metallic can (each metal can is tagged individually) as shown in Fig. 20.



Fig. 20. Read range measurement of half dozen pack of metallic can

The handheld reader was set to provide an equivalent isotropic radiated power (EIRP) of 630 mW. The measured read range for half dozen packs is more than 1.5 m from the top and more than 1 m for all other directions. This further elucidates that the proposed tag is a good candidate for tagging bulk of cans

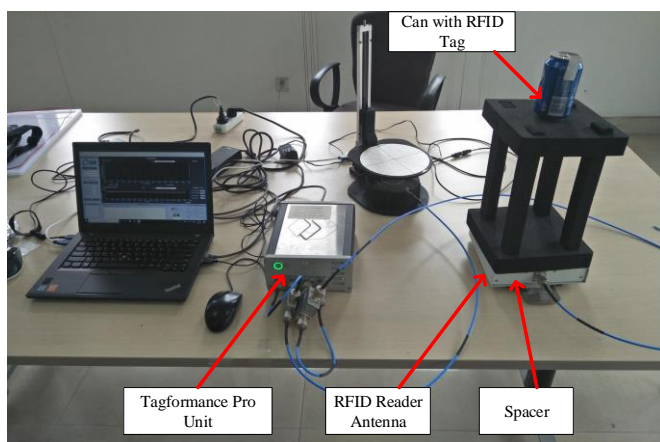


Fig. 18. Read range measurement set up based on Tagformance pro device from Voyantic Company

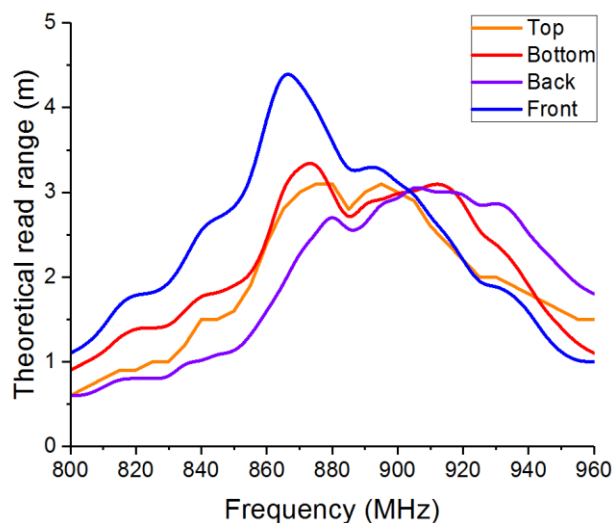


Fig. 19. Read range measurement using Tagformance based setup

VI. COMMERCIAL TESTING OF THE PROPOSED SYSTEM

A proof of the significance of proposed tag was made by testing it in a commercial application and demonstrates the idea of automatic billing of metallic cans along with some other products. The tagged metallic cans placed in a refrigerator set up used in this automatic billing experiment. This experiment shows a potential to revolutionize the IoT industry and supply chain management by providing item-level tracking of goods for effective decision-making. Fig. 21 describes the whole process of buying a product from smart refrigerator.

The customer with his smart phone (with installed online payment APP such Wechat or Alipay commonly used in China) scan QR code using online payment applications to open the door of refrigerator. The customer can pick any product from refrigerator. After closing the door of refrigerator, the RFID reader counts the no. of products and subtract the products picked by customer, and the payment is automatically deducted from his online payment account. The information of remaining products transferred to retailer by internet enabled RFID reader.

Moreover, the detailed schematic diagram of refrigerator set up is shown in Fig. 22. The refrigerator set up consists of shelves that contain RFID reader antennas (4-dBi circular polarized antenna). Array of four reader antennas is placed under each shelf. The above portion of refrigerator consists of LCD that was used to display the information about different products and to display the QR code to open the door of the refrigerator using online payment applications such as WeChat and Alipay. Moreover, the space behind the LCD was efficiently used to place the RFID reader setup (Impinj R420). Fig. 23 shows actual set up used for commercial testing of proposed RFID tag. We mount the ICE1 on 40 metallic cans containing different beverage drinks. The price and the drink types were encoded into EPC of each tag's microchip. The metallic cans with proposed RFID tag were placed on shelves inside the refrigerator (as shown in a subset of Fig. 23).

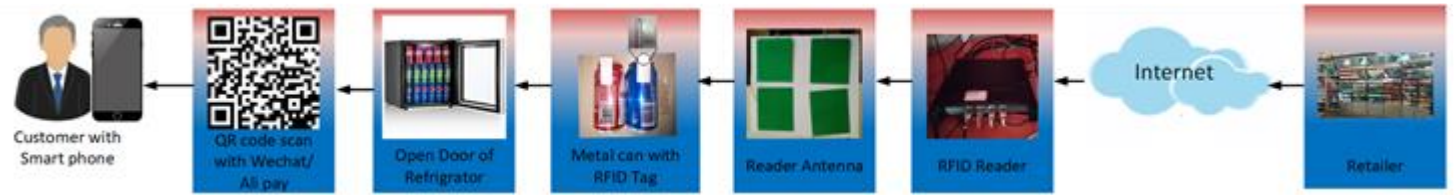


Fig. 21. Read range measurement of half dozen pack of metallic can

For automatic billing experiment, the customers can scan the QR code displayed on the screen and open the door of the refrigerator. The customers can pick any beverage drink (packed in a metallic can) of their own choice. After closing the door of the refrigerator, the amount of money will be automatically deducted from his online payment account.

The results of this experiment are shown below:

- 1) The automatic billing experiment was conducted by purchasing all the metallic cans one by one. In this case, the yield for automatic billing was 97.5 %. It means that only one metallic can out of 40 was miss read which may be due to some tag fabrication error or tag mounting error.
- 2) After that, an experiment of auto billing conducted by purchasing more than one metallic can after opening the door of the refrigerator, and in this case, the yield is about 92.5 % ,95 %, and 97.5% and for a first, second and third run of this experiment. This accuracy can be further improved by careful fabrication of tags. It means that 2 or 3 metallic cans were miss read due to some software or hardware discrepancies.
- 3) The hardware and software set can be further optimized to increase the yield of this commercial set up.
- 4) A unique feature is implemented using Algorithm 1, which counts the tagged products and generates an alert message for a retailer to place more products, if a certain product is less than a threshold (taken as 10 in our case). This feature envisages a future smart refrigerator for smart cities and IoT applications that can automatically place an order of required items to nearby store.
- 5) Another experiment is demonstrated by attaching a trash bin with refrigerator, an RFID reader antenna was housed at wall of trash bin; the trash bins is used for collecting the empty metallic cans and return a small incentive to the customers by reading the tag mounted on the beverage can by the same reader placed with in the refrigerator. And metallic cans can be reused in this manner, which saves cost and keep environment clean by developing the habits of customers to trash the empty cans into bins.

In Algorithm 1, the RFID Reader read all items from the refrigerator, when a customer takes some product from refrigerator, we count CountTotalProducts the all products from refrigerator and then minus the purchased products which store in total variable, if (total < 10) if any type of product less than 10 i.e., coca cola <10, then our system will

send notification to the retailer/shop keeper, the system sends message “soft drinks are less than 10 form the refrigerator no 1 and 8”. When user takes an item from refrigerator and closes the door of refrigerator, we used LockTheDoorOf Refrigerator () method for locking the door. If (UserBoughtProducts) than the amount will be automatically deducted from customer’s online payment account using method DetectAutomaticallyBalanceFromUserAccount(). If other customer wants to buy the products, then he/she needs to scan the QR code from his WECHAT/ALIPAY application to open the door of refrigerator and same process starts again.

Algorithm 1 RFID Reader Sends Requests to the Retailer

```

1: for Read RFID TAGs i do
2:   CountTotalProducts ← CalcluteProductsFromRefrigerator(i)
3:   total ← CountTotalProducts-userBoughtProduct
4:   if total < 10 then
5:     SendMessageToRetailer()
6:   end if
7:   if UserBoughtProducts then
8:     DetectAutomaticallyBalanceFromUserAccount()
9:     LockTheDoorOfRefrigerator()
10:  end if
11: end for
    
```

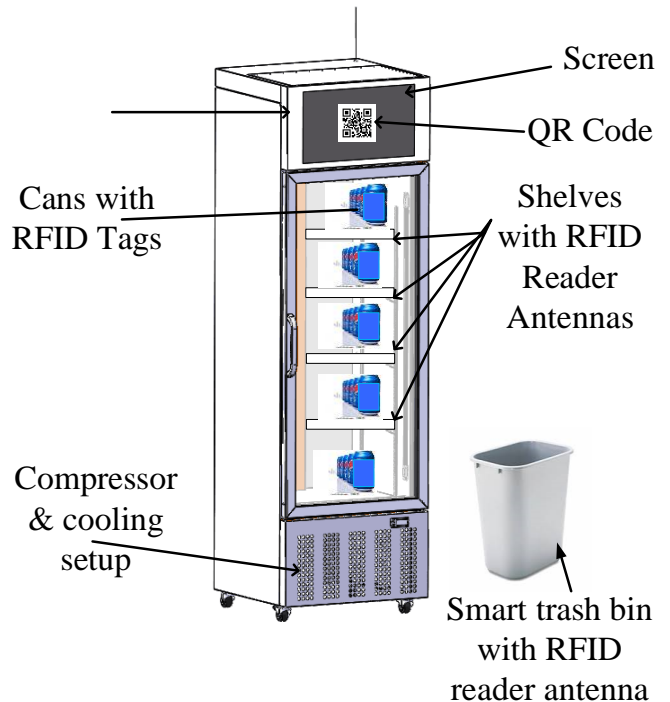


Fig. 22. Schematic diagram of refrigerator used in automatic billing experiment



Fig. 23. Commercial testing set up in operation for a metallic can with RFID

VII. CONCLUSION

In this paper, a low-cost smart refrigerator system with automatic billing and product restoring features was presented for the internet of things applications. To achieve an efficient and low-cost system for commercial deployments, a novel RFID tag antenna is designed for tagging the metallic cans with a real demonstration. The tag was proposed by exploiting the structure of metallic can as the main radiator using CMA. A characteristics mode of the metallic can with more radiation capacity (with more modal significant value) was excited by placing ICE at suitable position. A low-cost, flexible, conductive ink-jet printed antenna employed as an ICE. The proposed RFID tag is fulfilling the requirements of low cost, compact size. Furthermore, this tag antenna is fabricated by embedding inside thin layers of sprayed paint to hide or embed the tag inside the product and further to use the extra space provided by tag for logo printing and other advertisement printing purposes, which is pivotal for IoT. Therefore, this tag is a good candidate for tagging beverage metallic cans on a large scale. The read range is measured using Tagformance Pro setup for one RFID equipped metallic can which was more than 2.5 m for all reading directions. To investigate it further, the read range is measured using Handheld RFID Reader for one metallic can and a pack of half dozen metallic cans. The read range measured in case of half dozen metallic cans pack was 1 m, which shows potential application of this tag for conveyor belt applications. Finally, a low-cost RFID equipped smart

refrigerator system is demonstrated based on proposed tag design. An experiment of auto billing of the metallic can was performed to show the applicability of this system in the real world. The metallic cans can be restored by generating a product shortage alert message to nearby retailer. Additionally, the smart trash bin can provide cost effective and environment friendly solution by reutilizing the empty beverage cans. This experiment shows a potential to revolutionize the IoT industry and supply chain management by providing item-level tracking of goods for effective decision-making.

ACKNOWLEDGMENT

The Authors would like to thank Antenna Wireless Experts (www.designchn.com) for giving their resources for antenna fabrication and commercial testing. Also, the author would like to Thank Mr. Jiang Jianjun from Chengdu Push Information and Information cooperation for providing facilities for read range testing.

REFERENCES

- [1] C. Zhang and Y. Xie, "The Closed-form Solution of Frequency Shift for a HF RFID Coil Antenna in Metallic Environments," *IEEE Internet Things J.*, vol. 5, no. 5, pp. 1–1, 2018.
- [2] Y. Pang, H. Ding, J. Liu, Y. Fang, and S. Chen, "A UHF RFID based System for Children Tracking," *IEEE Internet Things J.*, vol. 4662, no. c, pp. 1–10, 2018.
- [3] Z. Meng, Z. Wu, and J. Gray, "RFID-based Object-Centric Data Management Framework for Smart Manufacturing Applications," *IEEE Internet Things J.*, vol. PP, no. APRIL, pp. 1–1, 2018.
- [4] W. M. Griggs, R. Verago, J. Naoum-Sawaya, R. H. Ordonez-Hurtado, R. Gilmore, and R. N. Shorten, "Localising Missing Entities using Parked Vehicles: An RFID-Based System," *IEEE Internet Things J.*, vol. 5, no. 5, pp. 1–1, 2018.
- [5] R. Li et al., "IoT applications on Secure Smart Shopping System," vol. 4662, no. c, pp. 1945–1954, 2017.
- [6] B. S. Çiftler, A. Kadri, and I. Güvenç, "IoT Localization for Bistatic Passive UHF RFID Systems with 3-D Radiation Pattern," *IEEE Internet Things J.*, vol. 4, no. 4, pp. 905–916, 2017.
- [7] A. Attaran and R. Rashidzadeh, "Chipless Radio Frequency Identification Tag for IoT Applications," *IEEE Internet Things J.*, vol. 3, no. 6, pp. 1310–1318, 2016.
- [8] M. S. Khan, M. S. Islam, and H. Deng, "Design of a reconfigurable RFID sensing tag as a generic sensing platform toward the future Internet of things," *IEEE Internet Things J.*, vol. 1, no. 4, pp. 300–310, 2014.
- [9] S. Amendola, R. Lodato, S. Manzari, C. Occhiuzzi, and G. Marrocco, "RFID technology for IoT-based personal healthcare in smart spaces," *IEEE Internet Things J.*, vol. 1, no. 2, pp. 144–152, 2014.
- [10] S. Chen, H. Xu, D. Liu, B. Hu, and H. Wang, "A Vision of IoT: Applications, Challenges, and Opportunities with China Perspective," *IEEE Internet Things J.*, vol. 1, no. 4, pp. 1–1, 2014.
- [11] G. Marrocco, S. Amendola, M. C. Caccami, A. Caponi, L. Catarinucci, and others "RFID & IoT: A Synergic Pair," no. 8, pp. 1–21, 2015.
- [12] A. Zanella, N. Bui, A. Castellani, L. Vangelista, and M. Zorzi, "Internet of Things for Smart Cities," *IEEE Internet Things J.*, vol. 1, no. 1, pp. 22–32, 2014.
- [13] E. Perret, S. Tedjini, and R. S. Nair, "Design of antennas for UHF RFID tags," *Proc IEEE*, vol. 100, no. 7, pp. 2330–2340, 2012.
- [14] D. M. Dobkin, *Te RF in RFID.UHF RFID in Practice*, Elsevier, Newnes, MA, USA, 2nd edition, 2013.
- [15] S. Shao, R. J. Burkholder, and J. L. Volakis, "Design approach for robust UHF RFID tag antennas mounted on a plurality of

- dielectric surfaces [antenna designer's notebook],” *IEEE Antennas Propag Mag*, vol. 56, no. 5, pp. 158–166, 2014.
- [16] A. P. Sohrab, Y. Huang, M. N. Hussein, and P. Carter, “A Hybrid UHF RFID Tag Robust to Host Material,” *IEEE J Radio Freq Identif*, vol. 1, no. 2, pp. 163–169, 2017.
- [17] H. Li, J. Zhu, and Y. Yu, “Compact Single-Layer RFID Tag Antenna Tolerant to Background Materials,” *IEEE Access*, vol. 5, pp. 21070–21079, 2017.
- [18] A. Hamani, M. C. E. Yagoub, T. P. Vuong, and R. Touhami, “A novel broadband antenna design for UHF RFID tags on metallic surface environments,” *IEEE Antennas Wirel Propag Lett*, vol. 16, pp. 91–94, 2017.
- [19] H. D. Chen, S. H. Kuo, C. Y. D. Sim, and C. H. Tsai, “Coupling-feed circularly polarized RFID tag antenna mountable on metallic surface,” *IEEE Trans Antennas Propag*, vol. 60, no. 5, pp. 2166–2174, 2012.
- [20] J. H. Lu and B. S. Chang, “Planar Compact Square-Ring Tag Antenna with Circular Polarization for UHF RFID Applications,” *IEEE Trans Antennas Propag*, vol. 65, no. 2, pp. 432–441, 2017.
- [21] M. L. Ng, “Design of High Performance RFID Systems for Metallic Item Identification - Thesis,” Thesis, p. 267, 2008.
- [22] I. J. Garcia, A. Sharma, J.C. Batchelor, I. Angulo, A. Perallos and J. M. H Elmighani, “Sprayed Antenna on Cans for WLAN-RFID Tags,” *Microw. Opt. Technol. Lett.* vol. 55, no. 4, pp. 773–775, 2013.
- [23] T. S. Kaisha, RFID Beverage Can. Available: <https://ssl.tskg-hd.com/wp-content/uploads/sites/5/2015/03/20081104.pdf> [Accessed: 10-OCT-2018].
- [24] “TOYO SEIKAN.” [Online]. Available: <http://www.toyo-seikan.co.jp/e/>. [Accessed: 10-OCT-2018].
- [25] C. R. Park and K. H. Eom, “RFID label tag design for metallic surface environments,” *Sensors*, vol. 11, no. 1, pp. 938–948, 2011.
- [26] “Access This Premium Content - RFID Journal.” [Online]. Available: <https://www.rfidjournal.com/purchase-access?type=Article&id=3088&r=%2Farticles%2Fview%3F3088>. [Accessed: 14-May-2018].
- [27] R. F. Harrington and J. R. Mautz, “Theory of Characteristic Modes for Conducting Bodies,” *IEEE Trans Antennas Propag*, vol. 19, no. 5, pp. 622–628, 1971.
- [28] M. Cabedo-Fabres, E. Antonino-Daviu, A. Valero-Nogueira, and M. F. Bataller, “The theory of characteristic modes revisited: A contribution to the design of antennas for modern applications,” *IEEE Antennas Propag Mag*, vol. 49, no. 5, pp. 52–68, 2007.
- [29] Y. Gao, R. Ma, Q. Zhang, and C. Parini, “Design of very-low-profile circular UHF small antenna using characteristic mode analysis,” *IET Microwaves, Antennas Propag*, vol. 11, no. 8, pp. 1113–1120, 2017.
- [30] Y. Chen and C. F. Wang, “Characteristic Modes: Theory and Applications in Antenna Engineering,” *Charact Modes Theory Appl Antenna Eng*, pp. 1–269, 2015.
- [31] R. Martens, E. Safin, and D. Manteuffel, “Inductive and capacitive excitation of the characteristic modes of small terminals,” *LAPC 2011 - 2011 Loughborough Antennas Propag Conf*, no. November, pp. 4–7, 2011.
- [32] R. Martens, E. Safin, and D. Manteuffel, “Selective Excitation of Characteristic Modes On Small Terminals,” pp. 2492–2496, 2011.
- [33] D. Manteuffel and R. Martens, “Systematic design method of a mobile multiple antenna system using the theory of characteristic modes,” *IET Microwaves, Antennas Propag*, vol. 8, no. 12, pp. 887–893, 2014.
- [34] E. Antonino-Daviu, M. Cabedo-Fabrés, M. Ferrando-Bataller, and M. Gallo, “Design of a multimode MIMO antenna using the theory of characteristic modes,” *Radioengineering*, vol. 18, no. 4, pp. 425–430, 2009.
- [35] R. Rezaiesarlak and M. Manteghi, “Design of chipless RFID tags based on Characteristic Mode Theory (CMT),” *IEEE Trans Antennas Propag*, vol. 63, no. 2, pp. 711–718, 2015.
- [36] Z. Liang, J. Ouyang, F. Yang, and L. Zhou, “Design of License Plate RFID Tag Antenna Using Characteristic Mode Pattern Synthesis,” *IEEE Trans Antennas Propag*, vol. 65, no. 10, pp. 4964–4970, 2017.
- [37] Z. Liang, J. Ouyang, M. Gao, and X. Cui, “A Small RFID Tag Antenna for Metallic Object using Characteristic Mode,” pp. 533–534, 2017.
- [38] E. A. Elghannai and R. G. Rojas, “Modal-based approach to tune and enhance the frequency and dielectric bandwidth of a UHF-RFID tag antenna mounted on a dielectric substrate,” *IEEE Antennas Propag Soc AP-S Int Symp*, vol. 2015–Octob, pp. 161–162, 2015.
- [39] M. Capek, V. Losenicky, L. Jelinek, and M. Gustafsson, “Validating the Characteristic Modes Solvers,” *IEEE Trans Antennas Propag*, vol. 65, no. 8, pp. 4134–4145, 2017.